Stability of the light-induced hidden charge density wave state within the phase diagram of $1T$-$TaS_{2-x}Se_x$

L. Stojchevska,[1] P. Šutar,[1] E. Goreshnik,[2] D. Mihailovic,[1,3] and T. Mertelj[1,3,*]

[1]*Complex Matter Dept., Jozef Stefan Institute, Jamova 39, Ljubljana, SI-1000, Ljubljana, Slovenia*

[2]*Dept. of Inorganic Chemistry and Technology, Jozef Stefan Institute, Jamova 39, 1000 Ljubljana, Slovenia*

[3]*Center of Excellence on Nanoscience and Nanotechnology-Nanocenter (CENN Nanocenter), Jamova 39, 1000 Ljubljana, Slovenia*

(Received 8 June 2018; revised manuscript received 25 October 2018; published 16 November 2018)

The femtosecond transient optical spectroscopy is employed to study the relaxation dynamics of the equilibrium and hidden metastable charge-density-wave states in single crystals of $1T$-$TaS_{2-x}Se_x$ as a function of the Se doping x. Similar to pristine $1T$-TaS_2, the transition to a hidden phase is observed at low temperature after a quench with a single 50 fs laser pulse, in the commensurate Mott phase up to $x = 0.6$. The photo-induced hidden-phase formation is accompanied by a notable change in the coherent phonon spectra, and particularly the collective amplitude mode. While the temperature stability of the hidden phase is only slightly dependent on the Se content, the creation-threshold fluence strongly increases with Se content from 1 to ~4 mJ/cm^2, which is attributed predominantly to the change in optical absorption coefficient at the laser excitation wavelength, and not an increased barrier of the hidden state with increasing Se.

DOI: 10.1103/PhysRevB.98.195121

I. INTRODUCTION

The interplay of different degrees of freedom shapes the manifold of emergent electronic and structural ordered phases in low-dimensional systems with competing interactions. A marked example is the class of nonsemiconducting layered transition-metal dichalcogenides [1]. In this class, $1T$-TaS_2 is of particular interest due to the presence of a metastable hidden (H) charge-density-wave (CDW) state induced by short strongly nonequilibrium optical [2] or electrical [3–5] excitations.

In equilibrium, the pristine $1T$-TaS_2 shows a series of electronic phase transitions upon cooling from high temperature [6]. First, at $T_{IC} = 550$ K, a transition to an incommensurate CDW (IC) phase is observed. With further cooling, a first-order transition to a nearly commensurate (NC) phase at $T_{NC} = 350$ K results in formation of star-shaped-polaron clusters. Below $T_C = 183$ K, the system undergoes a first-order lock-in transition into a commensurate (C) phase where the polarons order commensurately with the underlying atomic lattice. Concurrently, after Brillouin zone folding due to the enlarged unit cell, the resulting narrow half-filled Ta $5d$ valence band splits due to the electronic correlations forming a ~300 meV Mott insulator gap [7,8]. Upon heating the C phase, an additional trigonal (T) phase is observed between the C and NC phases in the range $T_T = 220\,\text{K} < T < 280\,\text{K}$. The C Mott state can be suppressed by pressure [9] or chemical doping [10], leading to the superconducting [11,12] ground state.

The nonequilibrium dynamics of this compound have been under intensive investigation recently [2,13–18], leading to the discovery [2] of the low-temperature metastable H phase. The phase forms under strongly nonequilibrium conditions on a short timescale [19] and at low T the H phase is practically stable [2,3]. With increasing T, the characteristic relaxation time, τ_H, shows activated behavior $\tau_H^{-1} \propto \exp(-T_A/T)$, where T_A depends on the in-plane strain [3]. In all-optical transient reflectivity experiments in bulk samples, τ_H drops to the single scan timescale of ~30 min at $T \sim 70$ K [2,3]. From the point of view of possible memory applications, it would be desirable to improve the stability of the H state at higher T. Furthermore, the origin of metastability is still not fully understood, and it is thus of importance to investigate the influence of different external control parameters on its properties within the phase diagram of isovalent substituted $1T$-$TaS_{2-x}Se_x$.

In the present case, we introduce isovalent Se substitution for S: $1T$-$TaS_{2-x}Se_x$, which exerts a chemical strain and local buckling and introduces disorder. The introduction of the chemical strain and disorder strongly alters the electronic ground state of $1T$-$TaS_{2-x}Se_x$ [11,12]. With increasing x, the hysteresis related to the NC-C-T phase transitions broadens, with the C phase being pushed to lower T on cooling, up to $x \sim 0.8$, whereafter the C Mott-insulating ground state is suppressed and the superconducting ground state appears [11,12]. The broader hysteresis at low doping suggests that the free-energy barriers between the C, NC, and T phases increase with the doping. Since a high-enough free-energy barrier is crucial for the stability of the metallic H state, a possibility exists that Se doping also increases stability of the H state [20] at elevated temperatures. To test this hypothesis, we investigated the influence of the Se doping on the H-phase formation threshold and stability.

The collective mode spectral shifts in pristine $1T$-TaS_2 were previously investigated both in equilibrium and in the metastable H and T states by means of the transient reflectivity spectroscopy over a large range of temperatures [19]. Shifts in

*tomaz.mertelj@ijs.si

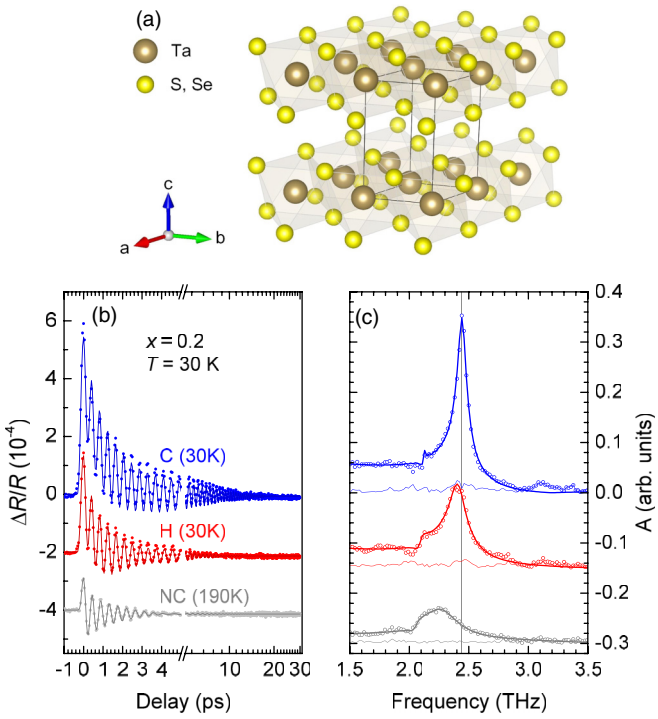

FIG.1. (a) The crystal structure of 1*T*-$TaS_{2-x}Se_x$. Transient reflectivity in different phases (b) with the corresponding FTA spectra (c). The thick lines are DCE fits. The thin lines in (c) correspond to the fit residua.

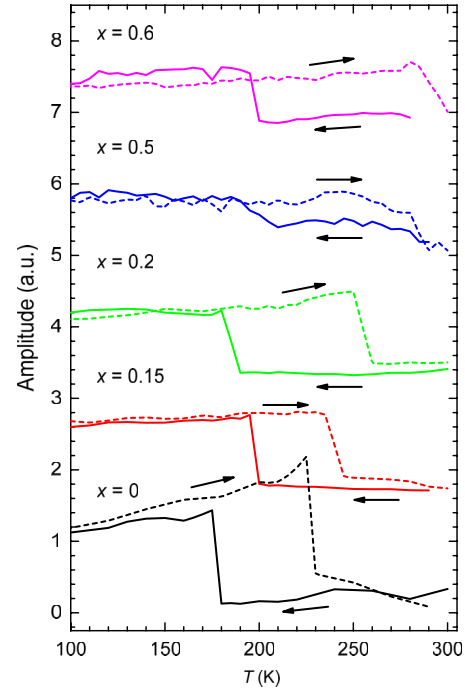

FIG. 2. Temperature dependence of the normalized transient reflectivity amplitude for different x. The data for different x are shifted verticaly while the arrows indicate cooling and warming scans.

the collective mode frequency, which presumably arise from changes of electronic structure accompanying the transition to the H state, were shown to be a useful fingerprint signature of the H state. Here we use this to investigate the stability of the optically induced H state in 1*T*-$TaS_{2-x}Se_x$ with $x \leqslant 0.6$.

II. EXPERIMENTAL

Single crystals of 1*T*-$TaS_{2-x}Se_x$ ($x = 0, 0.15, 0.2, 0.5$, and 0.6) were grown by means of the chemical transport reaction with iodine as the transport agent. Appropriate amounts of of Ta, S, and Se powders were put together with a small amount of I_2 into evacuated quartz ampules and placed into a three-zone temperature gradient furnace. The crystal growth was achieved by setting the temperature gradient across the ampules to 1000 °C – 800 °C for 216 h. Finally, ampules were quenched into water.

The obtained crystals in the form of mm-sized flakes were characterized by x-ray Laue diffraction while the Se content was determined by means of the standard energy-dispersive x-ray spectroscopy. For the optical measurements, the characterized crystals were mounted on a cold finger of a liquid-He flow optical cryostat equipped with CaF_2 windows and cleaved to expose fresh surface.

The optical pump-probe experiments were performed using a train of 50-fs laser pulses at 800 nm from a Ti: Sapphire laser system at a 250-kHz repetition rate. To ensure minimal heating and avoid switching into the H-phase, the pump and probe fluences were kept constant during all measurements and estimated to be $\mathcal{F}_p = 15\ \mu J/cm^2$ and $\mathcal{F}_{pr} = 0.5\ \mu J/cm^2$ for the pump and probe pulses, respectively.

For switching into the H phase, an additional single laser pulse at 800 nm with fluence $\mathcal{F}_{SW} = 1 - 5\ mJ/cm^2$ was picked from the pulse train by means of an acousto-optical modulator driven by a programmable wave-form generator.

III. RESULTS

In Fig. 1, we plot the characteristic transient reflectivity transients ($\Delta R/R$) in the the C, H, and NC phases in the $x = 0.2$ sample together with the Fourier transform amplitude (FTA) spectra. The C and NC phases differ strongly in the shape and the amplitude of the transients. To determine T_C and T_T, we first measured the T dependence of the transients during a cooling-warming cycle between 300 K and ~70 K . In Fig. 2, we show the normalized amplitude of the transients. Contrary to Refs. [10,11], we observe a weak increase of T_C with increasing x while T_T and the broadening of the hysteresis show a similar trend.

We further analyze the T-dependent transients using the displacive coherent excitation (DCE) model [19,21,22]. Contrary to $x = 0$ [19], where four modes were necessary to completely describe the line shape in the vicinity of the 2.45-THz amplitude (AM) mode, using only two modes at ~2.45 THz and ~2.1 THz together with the initial exponential relaxation enabled a fair fit to the data (see Fig. 1). The T-dependence of selected fit parameters for $x = 0.2$ sample is shown in Fig. 3. The 2.1-THz mode could be unambiguously fitted only below $T \sim 250$ K due to weaker intensities and strong broadening of the modes in the NC and T phases. Apart from the frequencies, the mode damping and the initial relaxation decay time τ, both show notable differences in different CDW phases.

Next, we checked for the presence of the H phase and determine the switching fluence at $T = 30$ K by measuring

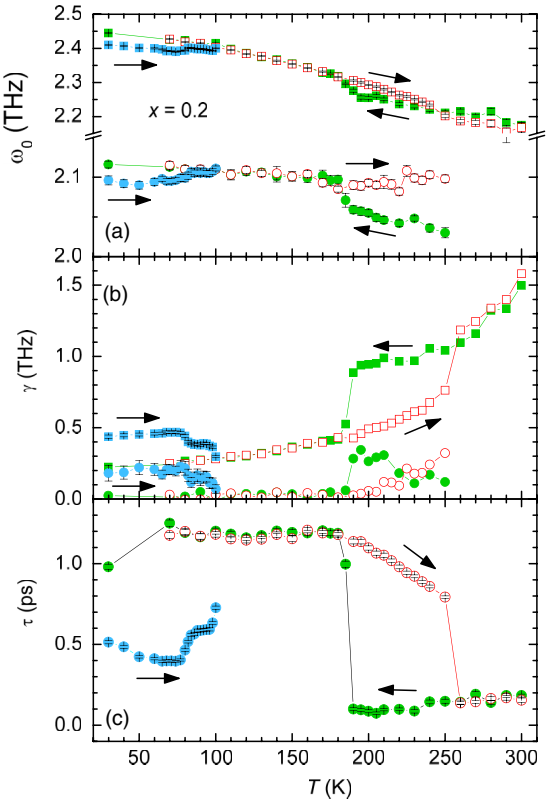

FIG. 3. Temperature dependence of the modes frequency, ω_0, damping, γ, and the initial relaxation time, τ, from the DCE fit for the $x = 0.2$ sample. Arrows indicate cooling/warming cycles. The blue symbols correspond to the warming scan in the H phase after application of an above-threshold optical switching pulse at $T = 30$ K.

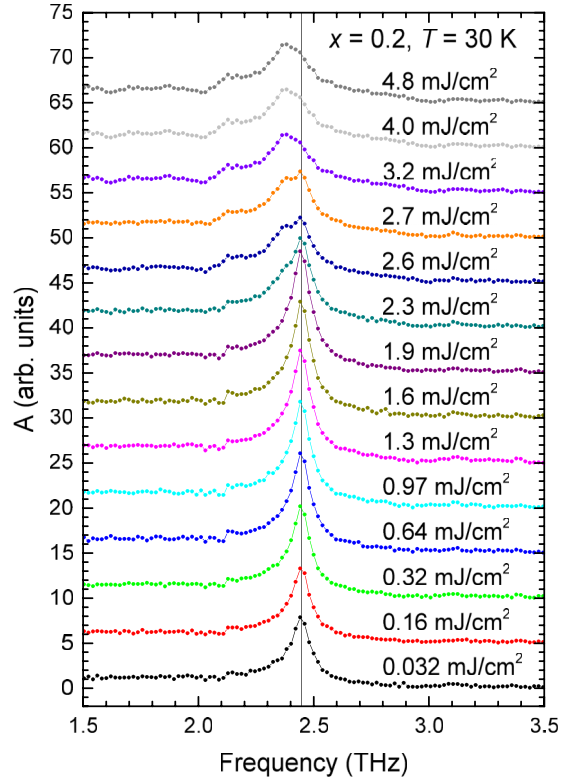

FIG. 4. The switching-pulse fluence dependence of the low-fluence transient reflectivity FTA spectra at 30 K for $x = 0.2$ sample.

a series of the low-fluence $\Delta R/R$ transients after an exposure to a single switching pulse of increasing fluence. An example sequence of the FTA spectra with increasing $\mathcal{F}_{SW}$ in the $x = 0.2$ sample is shown in Fig. 4. The H phase is characterized mainly by the softening of the strongest coherent mode from ~2.45 THz in the C phase to ~2.40 THz (at $T = 30$ K). The onset of the characteristic AM-mode spectral weight transfer [2] is observed at $\mathcal{F}_{SW} = 2.3$ mJ/cm^2. The switching is complete above $\mathcal{F}_{SW} = 2.7$ mJ/cm^2. In the intermediate $\mathcal{F}_{SW}$-interval, the spectral shape indicates incomplete switching with the presence of both C and H phases. The behavior is similar for all studied Se contents with the C- and H-phase spectra shown in Fig. 5. The corresponding threshold fluences, $\mathcal{F}_H$, are shown in Table I and Fig. 6(b). Here, $\mathcal{F}_H$ is defined as the minimal fluence where the completed spectral change is observed and it strongly increases with increasing x.

Once we had driven the system into the H phase, we investigated the T dependence of the reflectivity transients in the H phase. In these experiments, the H-phase transition was first triggered by the above-threshold fluence switching pulse at $T = 30$ K. Then the $\Delta R/R$ transients were recorded using a weak pump-probe sequence at an increasing T sequence until the C-phase transient response was observed.

The T dependence of the selected DCE-fit parameters in the H phase for the $x = 0.2$ sample is also shown in Fig. 3.

While the frequencies of both modes soften in the H phase, the modes decay faster (damping, γ, increases) and the initial

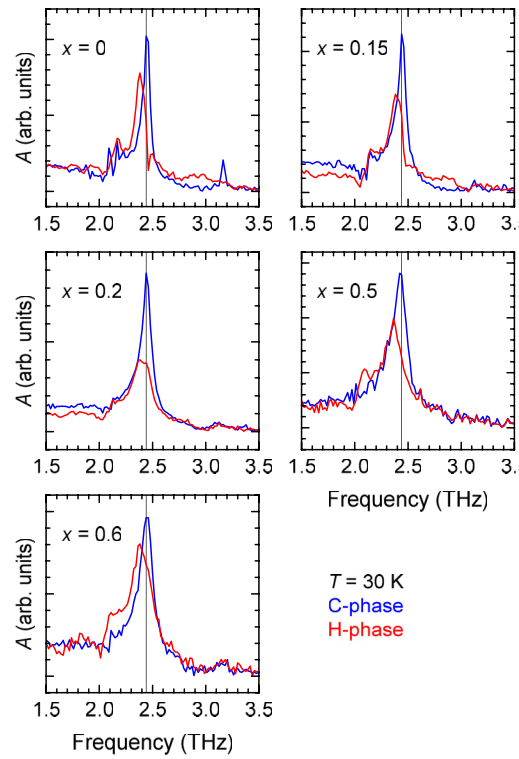

FIG. 5. Reflectivity transients FTA spectra in the C and H phase at $T = 30$ K for different Se doping levels, x.

TABLE I. The transition temperatures to/from the C state upon cooling (T_C) and warming (T_T), the threshold fluence, $\mathcal{F}_H$, for switching into the H phase at $T = 30$ K and the highest temperature T_H up to which the H phase persists on the timescale of the pump-probe scan (∼30 min) for different Se dopings.

x	T_C	T_T	$\mathcal{F}_H$ (@ 30 K)	T_H
0	180 K	225 K	1 mJ/cm^2	80 K
0.15	200 K	240 K	1.5 ± 0.1 mJ/cm^2	80 K
0.2	185 K	255 K	3 ± 0.2 mJ/cm^2	80 K
0.5	200 K	280 K	4 ± 0.4 mJ/cm^2	95 K
0.6	200 K	290 K	3.6 ± 0.4 mJ/cm^2	85 K

exponential relaxation time, τ, decreases. With increasing T, the strongest H-phase mode shows a similar softening as in the C phase (see also Fig. 7) until, at T_H, a recovery of the C-phase transient response is observed.[1]

$T_H \sim 80$ K also does not show a strong variation with x[2] except for $x = 0.5$ with $T_H \sim 95$ K [Table I and Fig. 6(a)]. In the $x = 0.5$ sample, we observe also a slightly softer AM mode in the C phase together with the softer corresponding mode in the H phase while for other dopings the frequency shift is observed only in the H phase.

[1]Since the stability time, τ_H, of the H phase strongly depends on T [3], T_H is set by the timescale of experiment [19], that was ∼30 min in the present case. On shorter timescale, the H phase can be readily observed at much higher T [19].

[2]In the $x = 0.2$ sample, we observe a two-step recovery of the C phase with the dominant recovery of the spectral shape at ∼80 K with the H-phase signature up to ∼100 K.

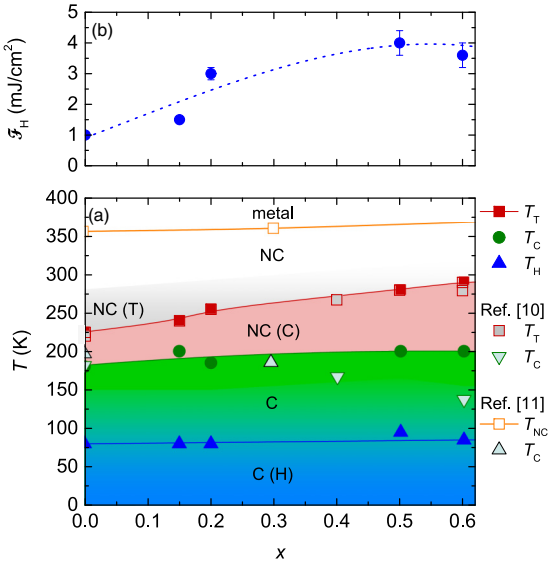

FIG. 6. (a) The H-phase $x - T$ stability diagram obtained from transient reflectivity data. The parentheses indicate warming. Open symbols are data from Refs. [10,11]. T_H is the temperature up to which the H phase is stable on the timescale of the pump-probe scan (∼30 min). The boundary between the T and NC phases on warming is tentative for $x > 0$ since it is not resolved in the transient reflectivity. (b) The H-phase threshold fluence as a function of x.

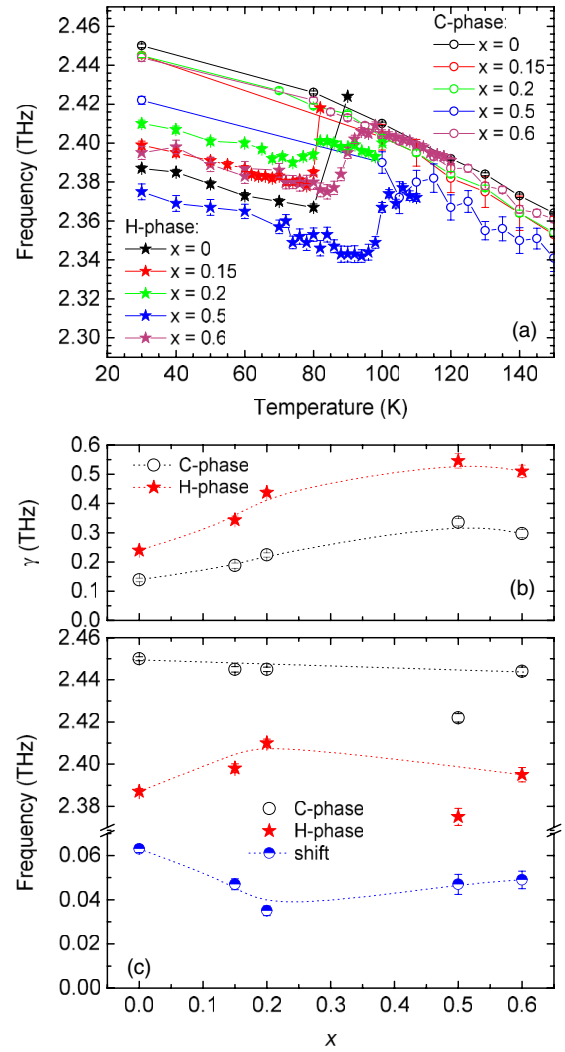

FIG. 7. (a) Temperature dependence of the 2.40-THz mode frequency on warming after switching into the H phase at 30K. The empty symbols refer to the frequency in the C phase. (b) Se doping dependence of the 2.4(5)-THz mode damping and (c) the frequency at $T = 30$ K in the C and H phases. The dotted lines are guide lines. The error bars correspond to the errors obtained from the DCE fit.

IV. DISCUSSION

Contrary to earlier results [10,11], our samples do not show a significant decrease of T_C with increasing x up to $x = 0.6$ (see Fig. 6). Since the NC → C transition is of first order, the pinning of the CDW in the NC phase by the Se disorder can play a significant role in supercooling the NC phase. Since the disorder can be sample dependent, the difference may be attributed to the sample-dependent disorder. On the other hand, our measurements were done under a weak continuous pump-probe optical excitation that can contribute to depinning and helps to trigger the transition at higher T. Moreover, in the optical measurements, the sample is kept at each measurement temperature for ∼40 min. Taking into account the temperature

step of $5-10$ K, this results in the average cooling/heating rate of less than 0.25 K/min that is ten times slower than for the published transport measurements [10]. The supercooling of the NC phase appears to be easier with the increasing Se content x.

Overall, the observed effect of Se substitution on the H phase is twofold. First, the transition temperature T_H increases only slightly or not at all, with increasing x as a result of increasing tensile strain [11] exerted by the larger Se substitution. We can qualitatively compare the chemical strain effect of Se ion substitution with in-plane differential strain experiments [23] with thin crystals of $1T$-TaS_2 on different substrates, where a tensile strain on cooling was found to empirically increase T_H. Taking into account that the a-lattice-constant increase by Se doping ($\sim$0.9% at $x = 0.6$) [11] is comparable to the maximum strain in the differential strain experiments [23] the two trends do not agree. Since in the present experiment the c lattice constant increases concurrently with a, the different behavior indicates that the interplane coupling contributes to the stability of the H phase.

The second effect is that the threshold fluence increases with increasing x. Pinning by the Se dopants would be expected to have an opposite effect in stabilizing the domain structure created in the switching process. Another possibility is that the absorption coefficient is changing with Se doping, changing the effective photoexcited carrier density. The photon absorption near 1.5 eV is related to a charge-transfer excitation between metal and chalcogen. It is therefore conceivable that the chalcogen substitution can have an effect on the imaginary part of the dielectric constant in this region. To our best knowledge, there is no data in the literature on the optical conductivity in $1T$-$TaS_{2-x}Se_x$, however, ARPES [24] data show significantly lower binding energy of the Se 4p-derived valence bands in $1T$-$TaSe_2$ in comparison to the S 3p-derived bands in 1T-TaS_2.

The effect of disorder may also have an influence if doping is associated with traps (e.g., on interstitials), thus reducing the photoinduced carrier density. A threefold increase in threshold fluence would require a significant number of traps, which we consider unlikely.

The frequency of the AM in the C phase does not show a significant x dependence while the corresponding mode frequency in the H phase shows a small[3] but detectable dependence [see Fig. 7(c)]. The absence of the shift in the C phase indicates that the AM-mode eigenvector does not include significant (S,Se) site displacements, as expected for the low-frequency modes. Since the corresponding mode observed in the H phase hardens slightly with increasing x, the shift can not be related to the larger Se mass. Considering that the broadening of the modes is most likely inhomogeneous and γ is an order of magnitude larger [see Fig. 7(b)] the origin of the shift can be attributed to a doping dependence of the Se inhomogeneity.

Moreover, in the $x = 0.5$ sample, a notable softening of $\sim$0.03 THz in comparison to the $x \neq 0.5$ samples is observed in both phases. This suggest a possibility of a Se ordering at this doping since $x = 0.5$ corresponds to a commensurate 25% filling of the triangular (S,Se) site lattice. The ordering, however, can not be long range since the mode linewidth is the largest at this doping. Nevertheless, the slight increase of the the H-phase stability at $x = 0.5$ could be tentatively linked to enhanced pinning of the H-phase domain walls by partially ordered rows of Se ions.

V. CONCLUSIONS

We demonstrated ultrafast-laser-pulse triggered transition of $1T$-$TaS_{2-x}Se_x$ system to the hidden photo-induced state over a major portion of the Mott-phase region ($x \leqslant 0.6$) and established the H-phase $x - T$ stability diagram.

The threshold fluence for the ultrafast transition into the H state significantly increases with increasing x from $\mathcal{F}_H \sim 1$ mJ/cm^2 at $x = 0$ to $\mathcal{F}_H \sim 4$ mJ/cm^2 at $x = 0.5$. The increase is attributed to the decrease of the absorption coefficient due to the chalcogen p-derived valence band shift upon Se substitution.

The hypothesis that the barrier for the thermal H phase to C-phase transition could be modified by the Se doping is rejected since the high temperature stability of the H phase is not significantly influenced by the Se doping despite a much larger effect on the stability of the equilibrium C phase during warming.

An exception is the $x = 0.5$ Se doping where the slight increase of the the H-phase stability concurrent with the AM mode softening is tentatively linked to partial Se-ion ordering. This suggests that a possible route for increasing the high-temperature stability of the H phase in the $1T$-TaS_2 system is through introduction of ordered pinning centers.

ACKNOWLEDGMENTS

The authors acknowledge the financial support of Slovenian Research Agency (Research Core Funding No. P1-0040) and European Research Council Advanced Grant TRAJECTORY No. GA 320602 for financial support. L.S. would also like to acknowledge support by Slovenian Ministry of Education, Science and Sport, ULTRA-MEM-Device Project No. 2013-IJS-731.

[3] An order of magnitude smaller than γ.

[1] J. A. Wilson, F. Di Salvo, and S. Mahajan, Adv. Phys. **24**, 117 (1975).

[2] L. Stojchevska, I. Vaskivskyi, T. Mertelj, P. Kusar, D. Svetin, S. Brazovskii, and D. Mihailovic, Science **344**, 177 (2014).

[3] I. Vaskivskyi, J. Gospodaric, S. Brazovskii, D. Svetin, P. Sutar, E. Goreshnik, I. A. Mihailovic, T. Mertelj, and D. Mihailovic, Sci. Adv. **1**, e1500168 (2015).

[4] M. J. Hollander, Y. Liu, W.-J. Lu, L.-J. Li, Y.-P. Sun, J. A. Robinson, and S. Datta, Nano Lett. **15**, 1861 (2015).

[5] I. Vaskivskyi, I. Mihailovic, S. Brazovskii, J. Gospodaric, T. Mertelj, D. Svetin, P. Sutar, and D. Mihailovic, Nat. Commun. **7**, 11442 (2016).
[6] R. E. Thomson, B. Burk, A. Zettl, and J. Clarke, Phys. Rev. B **49**, 16899 (1994).
[7] P. Fazekas and E. Tosatti, Philos. Mag. B **39**, 229 (1979).
[8] B. Dardel, M. Grioni, D. Malterre, P. Weibel, Y. Baer, and F. Lévy, Phys. Rev. B **46**, 7407 (1992).
[9] B. Sipos, A. F. Kusmartseva, A. Akrap, H. Berger, L. Forró, and E. Tutiš, Nat. Mater. **7**, 960 (2008).
[10] F. Di Salvo, J. Wilson, B. Bagley, and J. Waszczak, Phys. Rev. B **12**, 2220 (1975).
[11] Y. Liu, R. Ang, W. Lu, W. Song, L. Li, and Y. Sun, Appl. Phys. Lett. **102**, 192602 (2013).
[12] R. Ang, Y. Miyata, E. Ieki, K. Nakayama, T. Sato, Y. Liu, W. J. Lu, Y. P. Sun, and T. Takahashi, Phys. Rev. B **88**, 115145 (2013).
[13] J. Demsar, L. Forró, H. Berger, and D. Mihailovic, Phys. Rev. B **66**, 041101(R) (2002).
[14] N. Dean, J. C. Petersen, D. Fausti, R. I. Tobey, S. Kaiser, L. V. Gasparov, H. Berger, and A. Cavalleri, Phys. Rev. Lett. **106**, 016401 (2011).
[15] L. Perfetti, P. A. Loukakos, M. Lisowski, U. Bovensiepen, H. Berger, S. Biermann, P. S. Cornaglia, A. Georges, and M. Wolf, Phys. Rev. Lett. **97**, 067402 (2006).
[16] K. Haupt, M. Eichberger, N. Erasmus, A. Rohwer, J. Demsar, K. Rossnagel, and H. Schwoerer, Phys. Rev. Lett. **116**, 016402 (2016).
[17] C. Laulhé, T. Huber, G. Lantz, A. Ferrer, S. O. Mariager, S. Grübel, J. Rittmann, J. A. Johnson, V. Esposito, A. Lübcke, L. Huber, M. Kubli, M. Savoini, V. L. R. Jacques, L. Cario, B. Corraze, E. Janod, G. Ingold, P. Beaud, S. L. Johnson, and S. Ravy, Phys. Rev. Lett. **118**, 247401 (2017).
[18] M. Ligges, I. Avigo, D. Golež, H. Strand, Y. Beyazit, K. Hanff, F. Diekmann, L. Stojchevska, M. Kalläne, P. Zhou *et al.*, Phys. Rev. Lett. **120**, 166401 (2018).
[19] J. Ravnik, I. Vaskivskyi, T. Mertelj, and D. Mihailovic, Phys. Rev. B **97**, 075304 (2018).
[20] K. Sun, S. Sun, C. Zhu, H. Tian, H. Yang, and J. Li, Sci. Adv. **4**, eaas9660 (2018).
[21] H. J. Zeiger, J. Vidal, T. K. Cheng, E. P. Ippen, G. Dresselhaus, and M. S. Dresselhaus, Phys. Rev. B **45**, 768 (1992).
[22] L. Stojchevska, M. Borovšak, P. Foury-Leylekian, J.-P. Pouget, T. Mertelj, and D. Mihailovic, Phys. Rev. B **96**, 035429 (2017).
[23] D. Svetin, I. Vaskivskyi, P. Sutar, E. Goreshnik, J. Gospodaric, T. Mertelj, and D. Mihailovic, Appl. Phys. Exp. **7**, 103201 (2014).
[24] F. Clerc, M. Bovet, H. Berger, L. Despont, C. Koitzsch, O. Gallus, L. Patthey, M. Shi, J. Krempasky, M. Garnier *et al.*, J. Phys.: Condens. Matter **16**, 3271 (2004).